Journal of Geophysical Research Solid Earth

Supporting Information for

Rise of Great Lakes surface water, sinking of the upper Midwest of the United States, and viscous collapse of the forebulge of the former Laurentide ice sheet

Donald F. Argus[1], Benjamin Ratliff[2], Charles DeMets[2], Adrian A. Borsa[3], David N. Wiese[1], Geoffrey Blewitt[4], John W. Crowley[5], Hilary R. Martens[6], Corné Kreemer[4], Felix W. Landerer[1]

[1]Jet Propulsion Laboratory, California Institute of Technology, Pasadena, CA, USA
Donald.F.Argus@jpl.nasa.gov (818) 216 3983

[2]Department of Geoscience, University of Wisconsin, Madison, WI, USA

[3]Scripps Institution of Oceanography, University of California, San Diego, La Jolla, CA, USA

[4]Nevada Geodetic Laboratory, Nevada Bureau of Mines and Geology, University of Nevada, Reno, NV, USA

[5]Canadian Geodetic Survey, National Resources Canada, Ottawa, Ontario, Canada

[6]Department of Geosciences, University of Montana, Missoula, MT, USA

This supporting information consists of supplementary text on data and methods and Figures S1 to S17.

Supplementary Material on Data and Methods

GPS

1 GPS Positioning.

Series of position as a function of time of 3658 GPS sites in North America are from Nevada Geodetic Laboratory (NGL) [Blewitt et al. 2018]. Scientists at Jet Propulsion Laboratory (JPL) first estimate satellite orbits and clocks and positions of about 80 GPS sites each day from 1994 to 2019 in the IGS14 reference frame (in JPL's 'Repro 3.0', which follows the IGS Repro 2 standards except for the reference frame) using the technique of Zumberge et al. [1997]. NGL scientists next estimate the positions of GPS sites each day using the GipsyX software program pppZap/gd2e.py [Blewitt et al. 2018, Bertiger et al. 2020]. In total 44,805,783 positions on distinct days are estimated at 18,414 GPS sites. NGL then transforms GPS positions from a loosely constrained reference frame into the IGS14 frame [Rebischung et al. 2016] using JPL's 'X files', which on each day is a similarity transformation consisting of a translation, a rotation, and a scale.

NGL estimated positions using improved techniques. The troposphere model consists of dry and wet zenith delays from ECMWF and the VMF1 mapping function [Boehm et al. 2006] interpolated to each GPS site every 5 minutes, with the data weighted by elevation angle; a wet zenith bias parameter and two gradient parameters are furthermore estimated also every 5 minutes as random walk stochastic processes. The ionosphere model is calculated on the basis of dual frequency ionospheric correction, JPL's total electron content (TEC) in ionosphere exchange (IONEX) format, and the 12th generation of the International Geomagnetic Reference Frame (IGRF). The satellite antenna phase center variations are from Rebischung and Schmid [2016, igs14.atx].

We fit a position, a velocity, and a sinusoid with a period of 1 year to GPS data from 1994 to 2019 following the methods of Argus et al. [2010, 2017]. We estimated offsets

when needed, whether they be at the time of logged antenna substitutions, earthquakes, or of unknown source (in most instances suspected to be unlogged antenna substitutions). Earthquake offsets and postseismic transients were assumed to negligible in the eastern U.S.in the eastern U.S. In the western U.S., we estimated coseismic offsets and deleted all GPS positions biased by postseismic transients of the 2012 M 7.8 Haida Gwaii, 2010 M 7.2 Baja, 1999 M 7.1 Hector Mine, 2003 M 6.5 San Simeon, 2014 M 6.0 South Napa, and M 6.0 Parkfield earthquakes.

The median root mean square dispersion of positions at 1530 GPS sites in eastern North America are, in the east, north, and up component, 1.5 mm, 1.6 mm, and 5.6 mm (with 15 and 85 percentile values of 4.1 mm and 5.9 mm).

The accuracy of NGL's GPS positions improved just prior to this study, as evident in a 15 per cent reduction in root mean square (rms) dispersion [Blewitt et al. 2019]. This advance resulted from JPL's re-estimation of all satellite orbits and clocks from 1994 to 2019 (in Repro 3.0 relative to IGS14, as opposed to in Repro 2.1 in IGS08) and from NGL redetermination of 18,400 site positions using improved techniques (as described in the preceding paragraph). NGL's adoption of wet and dry zenith delays each day from ECMWF and the VMF1 mapping function resulted in a second 15 per cent reduction in the rms dispersion in the up component after atmospheric loading is removed (as described in the next paragraph).

2. Removing Atmosphere and Non-Tidal Ocean Loading.

We removed elastic vertical displacements produced by changes in atmosphere and non-tidal ocean loading using values calculated by the German Center for Geoscience [Dill and Dobslaw 2013]. Dill and Dobslaw [2013] calculate solid Earth's elastic response to changes in non-tidal atmosphere mass in model ERA Interim from the (ECMWF) European Center for Medium-Range Weather Forecasting [Dee et al. 2011]. Dill and Dobslaw [2013] calculate elastic displacements relative to the (CF) center of figure of Earth using the Green's functions of Wang et al. [2012, for the ak135 Earth

structure]. We interpolate GFZ's values at 0.5° intervals of latitude and longitude to the location of the GPS site and we each day take the mean of eight GFZ's values specified every 3 hours. Removing the elastic displacements reduced the root mean square dispersion in the up component by 15 percent (to a median of 4.8 mm, with 15 and 85 percentile values of 4.1 mm and 5.9 mm).

We corrected for elastic displacements produced by changes in atmosphere mass using Green's loading functions relative to mean position of Earth's surface (CF). In the long term, the mass center (CM) of Earth (consisting of solid Earth, oceans, ice, and atmosphere) defines ITRF2014. In the seasons, the mean position of Earth's surface (CF) defines solid Earth because ITRF does not allow there to be seasonal oscillations in CM. The displacement between CF and the mass center of solid Earth (CE) is minuscule [cf. Dong et al. 2002]. We maintain that the velocity between CM and CE may be significant but must be small, no more than 0.3 mm/yr [Argus 2007, 2012].

The predicted elastic displacement of GPS sites produced by changes in Great Lakes water varies ever so slightly between the CF, CE, and CM reference frames. GPS site MICX is predicted to fall by 16.7 mm relative to CE in elastic response to the the 285 km^3 of Great Lakes water gain from Oct 2012 to Oct 2019. MICX's predicted elastic displacement from 2012 to 2019 relative to CF differs from that relative to CE by just 0.008 mm. MICX's elastic displacment relative to CM differs from that relative to CE by 0.304 mm. We calculated solid Earth's elastic response relative to CF, CM, and CE using the Green's loading functions in Martens et al. [2019]. The 0.304 mm displacement between CE and CM can also calculated to be the 285 x 10^{12} kg Great Lakes water gain divided by the 6 x 10^{24} kg mass of Earth, multiplied by Earth's 6371 x 10^3 m radius.

3. Distinguishing between elastic and porous response.

We distinguished GPS sites having an elastic response to change in mass load from those with a porous response following the method of Argus et al. [2014, 2017]. GPS

sites with a seasonal maximum vertical position around March are taken to be responding porously. In North America, groundwater filling the pores in silts, sands, and gravels causes an aquifer to expand and Earth's surface to attain a maximum around March. GPS sites subsiding faster than about 2 mm/yr are responding porously. Pumping of groundwater from an aquifer causes the aquifer to contract and Earth's surface to subside. In particular, five GPS sites in the Red Lake Peatland Scientific and Natural Area, Minnesota, are responding porously to fluctuations in groundwater, as evident in their big seasonal vertical oscillations with maximum vertical height around August.

4. Removing solid Earth's elastic response to changes in Great Lakes surface water.
We describe our method for removing solid Earth's elastic response to change in Great Lakes surface water in the main text.

5. Removing solid Earth's viscous response to unloading of the Late Pleistocene ice sheets.
We removed solid Earth's viscous response to unloading of the Late Pleistocene/early Holocene ice sheets using the ICE 6G/VM5a model [Peltier et al. 2015, 2018, Argus Fu Landerer 2014]. The 6G model well fits Holocene geologic relative sea level histories [e.g., Vacchi et al. 2018] and geodetic rates (mostly GPS) of site vertical motion throughout North America [Peltier et al. 2015].

GRACE

1. GRACE mass change.
Time series of change in total water storage at Earth's surface are from JPL's GRACE mascon determination [Release 6, Version 2, Wiese et al. 2016, Watkins et al. 2015]. Changes in total water storage each month from April 2002 to September 2019 are estimated in 3° x 3° mass elements at Earth's surface using GRACE and GRACE Follow On gravity measurements. Changes in atmosphere mass have been removed

using AOD1B [Release 6, Dahle et al. 2019], a model using the same ECMWF estimates of atmosphere mass used to correct the GPS positions.

2. Simulating GRACE measurement of surface change using a Gaussian function.
We simulated the mass change signature that GRACE sees at an altitude of 400 km using the Gaussian function [following Wahr et al. 1998]:

$$\exp\left((-x/\sigma)^2 / 2 \right) / \left(\sigma (2\pi)^{1/2} \right)$$

where x is the distance from an element of surface water change in the Great Lakes and σ is the fullwidth of the Gaussian distribution. Changes in Great Lakes surface water each month measured by water level gauges are specified at 1855 elements inside the five Great Lakes at 1/8° intervals of latitude and longitude.

Supplementary Figure Captions

Figure S1. Change in water levels in the five Great Lakes from Jan 1991 to Dec 2019 measured by water level gauges (dots with different colors signify the seasons). Change in Great Lake water levels estimated using satellite altimetry [USDA 2019] (black dots) nearly equals that measured by water level gauges. Vertical axes at left are in meters and are identical; vertical axes at right are in cubic kilometers and depend on Great Lake area.

Figure S2. Solid Earth's horizontal displacement in elastic response to increase in Great Lakes surface water volume from October 2012 to October 2019. Places in the Great Lakes drainage basin moved toward the Lakes 1–4 mm. Horizontal displacement is maximum at LCUR (3.9 mm) and PARY (3.9 mm).

Figure S3. Present-day rate of vertical motion (color gradations) reflecting solid Earth's viscous response to unloading of the Laurentide (Canadian) ice sheet 15 to 5 thousand years ago in glacial isostatic adjustment model ICE 6G/VM5a [Peltier et al. 2015, 2018, Argus et al. 2014]. The model fits nearly all available Holocene relative sea level histories and geodetic estimates of current vertical motion. Parts of Canada east and west of Hudson Bay are rising as fast as 14 mm/yr (red colors). The forebulge around the former ice sheet is now collapsing as fast as 2 mm/yr in the northern United States (blue colors).

Figure S4. Solid Earth's subsidence (blue to magenta color gradations) in elastic response to the increase in Great Lakes surface water volume from April 2013 to April 2016. Contours are at 3, 5, 10, and 15 mm of subsidence. The 4-letter abbreviations of the 24 GPS sites in Figs. S4, S5, and S6 are in yellow text. The 4-letter abbreviations of Canadian Base Network sites are in green text.

Figure S5. Vertical displacement each month of 10 GPS sites along or near the coast of Lake Superior. Elastic vertical displacement produced by changes in Great Lakes

surface water (green) is removed from vertical displacement observed with GPS (blue) to estimate vertical displacement reflecting phenomena other than Great Lakes loading (red). Viscous vertical displacement generated by glacial isostatic adjustment orange) is steady; the predictions of model ICE 6G/VM5a are plotted. The locations of the 10 GPS sites are shown in Fig. S4 (the 4-letter site abbreviations are in yellow text).

Figure S6. Vertical displacement each month of 10 GPS sites along or near the coast of Lake Michigan. Otherwise identical to Fig. S5.

Figure S7. Vertical displacement each month of 10 GPS sites along or near the coast of Lake Huron.

Figure S8. (a) Rise in surface water level (in m) in the five Great Lakes from April 2013 to April 2016 measured by water level gauges. (b) Change in Great Lakes surface water smeared by a Gaussian distribution of 334 km. (c) Change in total water storage from April 2013 to April 2016 observed with GRACE (JPL's mascon solution [Watkins et al. 2015, Wiese et al. 2016]). Change in equivalent water thickness in each 3° x 3° mascon is given in m. (d) Average in each 3° x 3° mascon of (diagram b) change in Great Lakes surface water smeared by a Gaussian of 334 km. (e) Change in total water minus mascon average of change in Great Lakes surface water smeared by a Gaussian distribution of 334 km (diagram b minus diagram d). Residual change in equivalent water thickness is less than 0.125 m in all places in the Great Lakes drainage basin. At bottom right in each of the five diagrams is water change in the Great Lakes basin (brown outline) in km^3.

Figure S9. (Left-hand column) Change in Great Lakes surface water smeared by Gaussian distributions with full widths of (1st page) 222 km, 334 km, 445 km and of (2nd page) 278 km, 334 km, and 389 km. (Right-hand column) Change in total water storage observed with GRACE minus change in Great Lakes surface water smeared by

the Gaussian distribution with the full width to the left. Residual water change in the Great Lakes drainage basin is smallest for a Gaussian full width of 334 km.

Figure S10. Areas that water change estimated from GRACE are averaged over in Fig. S11: the Great Lakes drainage basin (maroon), an area extending 167 km beyond the coast of the Great Lakes (sandy brown), and ten 3° x 3° mascons from JPL's GRACE solution (green).

Figure S11. Water change in the Great Lakes drainage basin are calculated using three different assumptions about the area of the basin (see Fig. S10). In Fig. 7, duplicated in this illustration, we calculate water change in the drainage basin using an area extending 167 km beyond the coast of the Great Lakes: (a) Change in total water in the Great Lakes basin estimated with GRACE (brown), (b) Change in water in the Great Lakes basin after removing Great Lakes surface water smeared by a Gaussian with a full width of 334 km (blue), (c) Change in water in the ground in the Great Lakes basin (violet) is inferred to be change in total water estimated with GRACE minus Great Lakes surface water minus a composite hydrology model (pink). In each of the three diagrams, the curves in yellow show water change calculated on the basis of the true Great Lakes drainage basin and the curves in green show water change calculated on the basis of ten 3° x 3° mascons. The estimates of water change do not depend strongly on the area chosen to represent the drainage basin. Assuming the Great Lakes Basin to be the ten mascons results in slightly greater water change than the area extending 167 km from the Great Lakes; taking the drainage basin to be the true Great Lakes basin defined by all rivers flowing into the Great Lakes results in slightly less water change.

Figure S12. Mean change in total water from October 1 to April 1 in (a) a composite hydrology model and (b) observed with GRACE after removing the Gaussian-smoothed realization of Great Lakes surface water change. Color gradations show the size of the oscillation in water (white is zero, blue to magenta depicts increasing water oscillation).

The sine component would be the entire seasonal oscillation if water were maximum in April. Contours are at 0.125 m and 0.25 m of peak-to-peak water oscillation. The composite hydrology model consists of snow in SNODAS and soil moisture in NLDAS–Noah. The mean oscillation in the Great Lakes drainage basin is given at top right for each diagram; the 15 percentile, median, and 85 percentile values of the oscillation in the drainage basin is given at bottom right.

Figure S13. Change in total water from April 2013 to April 2016 observed with GRACE after removing change in Great Lakes surface water smeared by a Gaussian with a full width of 334 km. Color gradations show the size of the oscillation in water (white is zero, blue to magenta depicts water gain, green to yellow depicts water loss). Contours are at –0.125 m, 0.125 m, and 0.25 m of change in equivalent water thickness.

Figure S14. Change in total water from October 2012 to October 2019 observed with GRACE after removing change in Great Lakes surface water smeared by a Gaussian with a full width of 334 km. Color gradations show the size of the oscillation in water (white is zero, blue to magenta depicts water gain, green to yellow depicts water loss). Contours are at –0.125 m, 0.125 m, and 0.25 m of change in equivalent water thickness.

Figure S15. Phasor diagram depicting seasonal vertical displacements observed with GPS (blue arrows), produced by Great Lakes surface water changes (red arrows), and predicted by water change estimated using GRACE (brown arrows). The length of an arrow signifies the peak-to-peak amplitude in the seasonal oscillation (values for some sites are given in mm). The direction of the arrow signifies the time of year of maximum vertical position as specified by the legend at top right.

Figure S16.
Phasor diagram of peak-to-peak seasonal vertical displacements estimated with GPS after removing Great Lakes elastic loading (blue arrows), in the composite hydrology

model (pink arrows), and predicted by water change estimated using GRACE after removing Great Lakes surface water change smeared by a Gaussian of 334 km (brown arrows). The length of an arrow signifies the peak-to-peak amplitude in the seasonal oscillation (values for some sites are given in mm). The direction of the arrow signifies the time of year of maximum vertical position as specified by the legend at top right.

Figure S17. Mean change in total water from October 1 to April 1 observed with GRACE after removing the Gaussian-smoothed realization of Great Lakes surface water change is depicted by the blue color gradations as specified in the legend (identical to Fig. S12). Phasor diagram of peak-to-peak seasonal vertical displacements estimated with GPS after removing Great Lakes loading (blue arrows), in the composite hydrology model (pink arrows), and predicted by water change estimated using GRACE after removing Great Lakes surface water change smeared by a Gaussian of 334 km (brown arrows) (identical to Fig. S16).

Figure S1

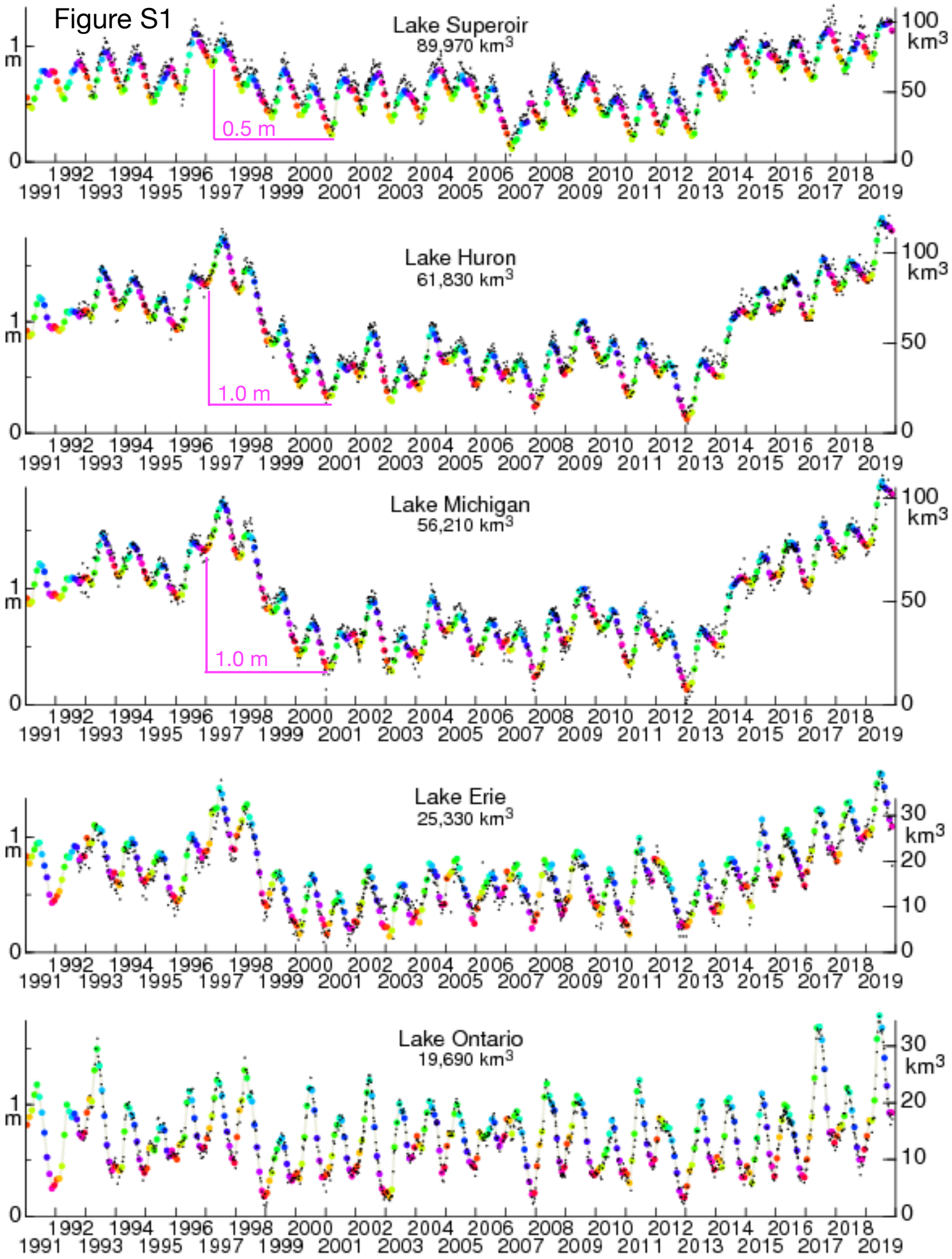
Lake Superoir
89,970 km3
0.5 m
Lake Huron
61,830 km3
1.0 m
Lake Michigan
56,210 km3
1.0 m
Lake Erie
25,330 km3
Lake Ontario
19,690 km3
1 m
0
100 km3
50
30 km3
20
10
1991 1992 1993 1994 1995 1996 1997 1998 1999 2000 2001 2002 2003 2004 2005 2006 2007 2008 2009 2010 2011 2012 2013 2014 2015 2016 2017 2018 2019

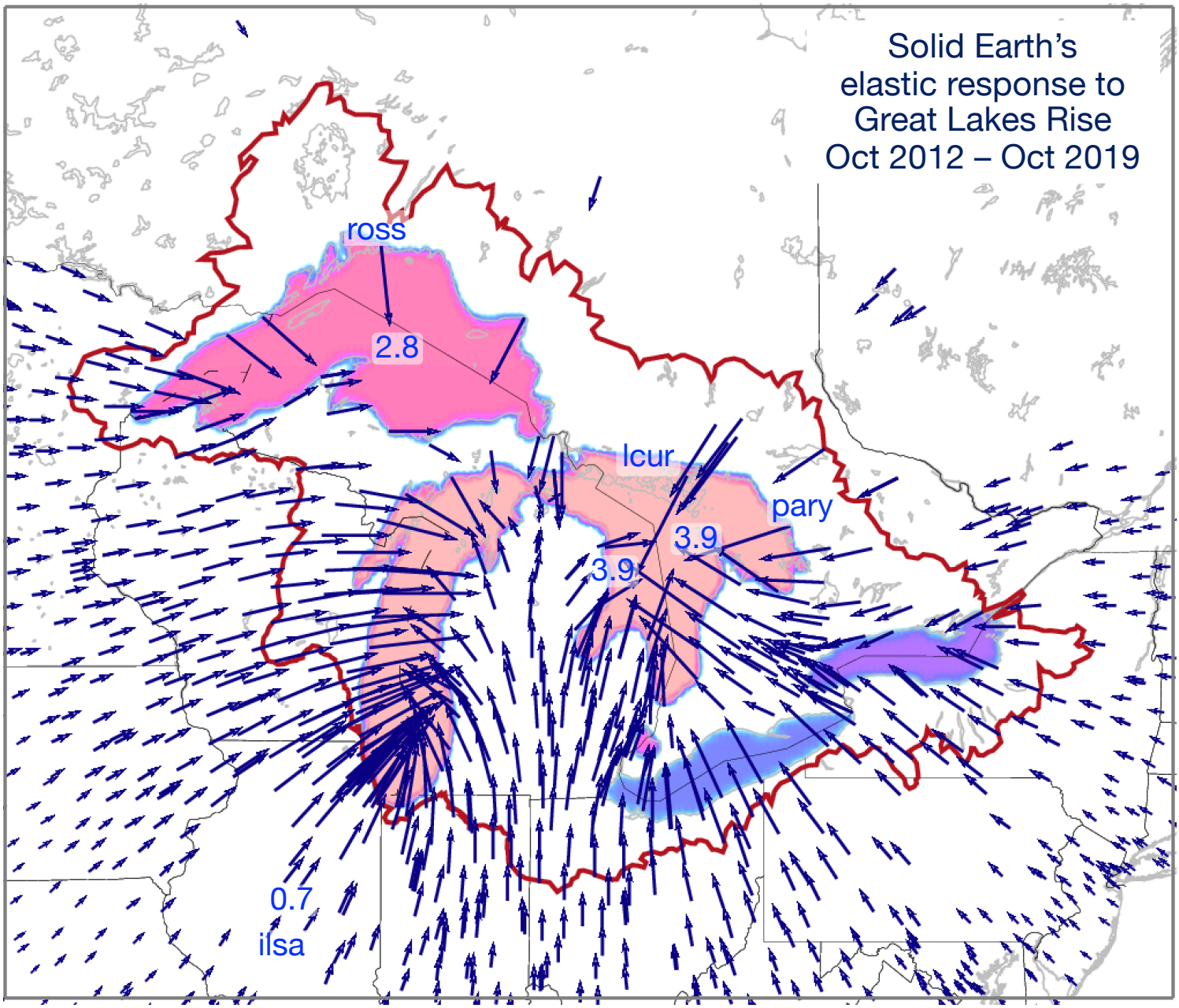
Solid Earth's
elastic response to
Great Lakes Rise
Oct 2012 – Oct 2019
ross
2.8
lcur
pary
3.9
3.9
0.7
ilsa

Figure S2

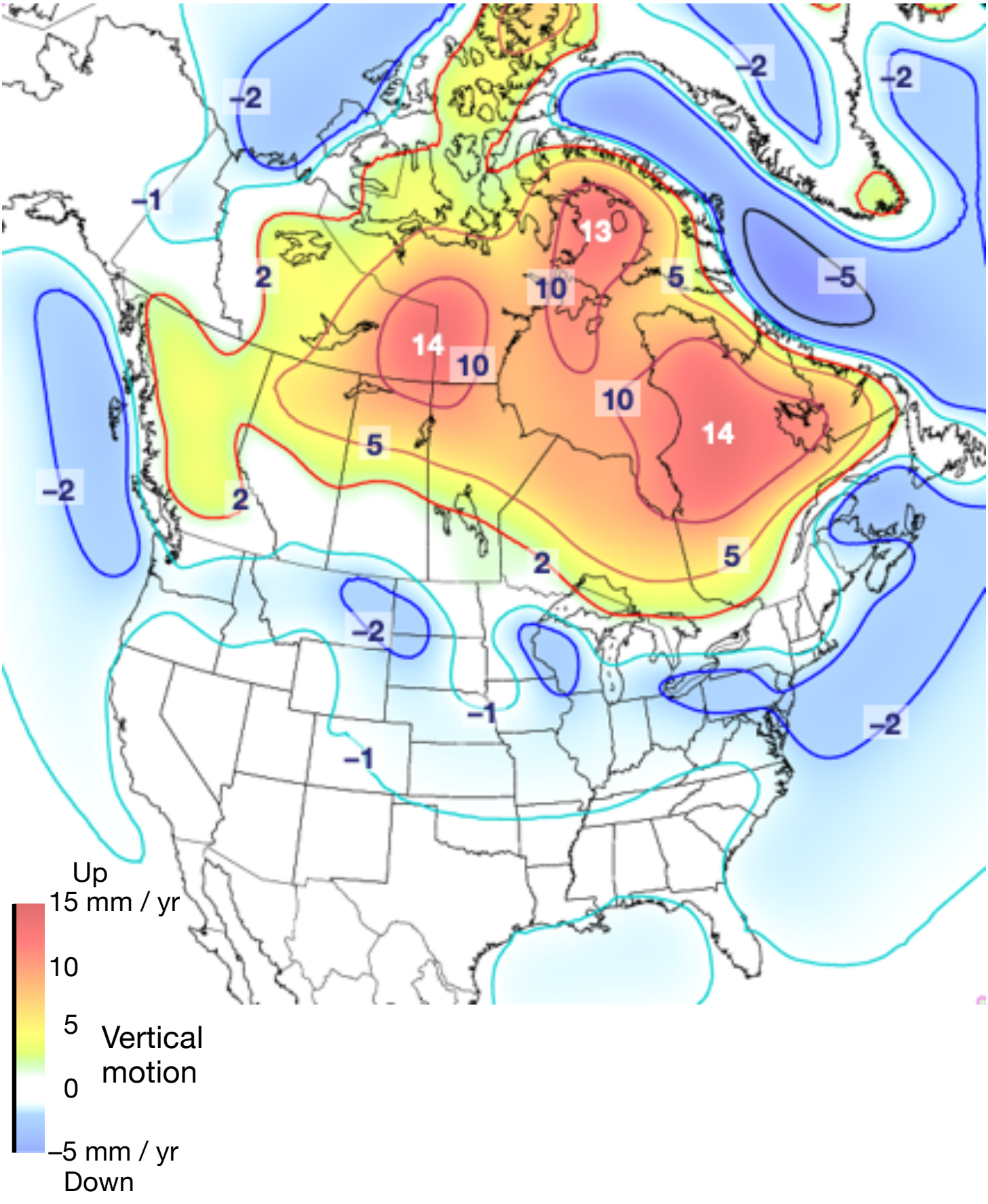

Figure S3

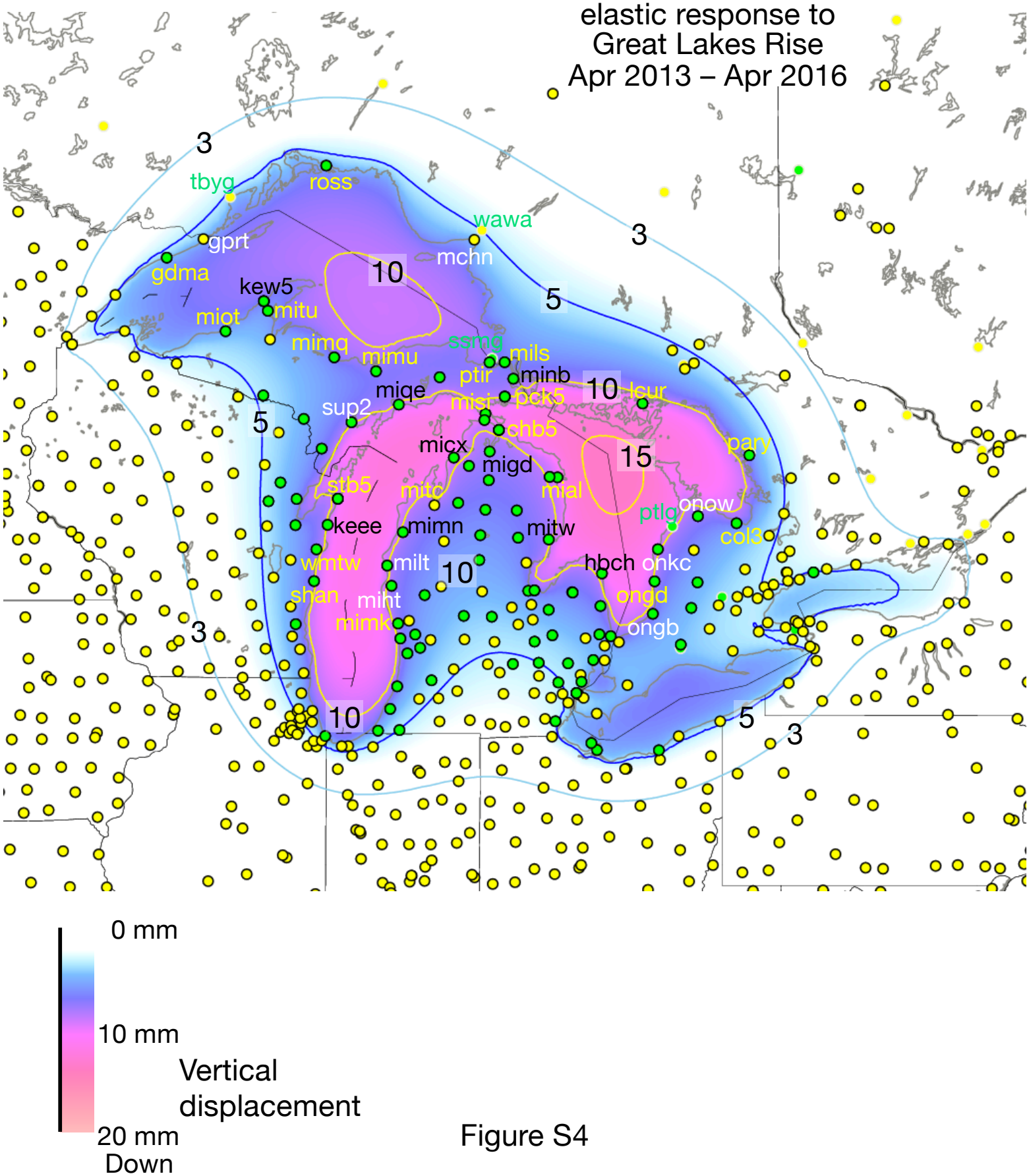
Solid Earth's
elastic response to
Great Lakes Rise
Apr 2013 – Apr 2016
3
tbyg
ross
wawa
3
gprt
mchn
gdma
10
kew5
5
mitu
miot
mimq
mimu
ssmg
mils
ptir
minb
10
lcur
miqe
misi
pck5
sup2
5
chb5
micx
pary
15
migd
stb5
mitc
mial
ptlg
onow
keee
mimn
mitw
col3
wmtw
milt
10
hbch
onkc
shan
miht
ongd
mimk
ongb
3
10
5
3
0 mm
10 mm
Vertical
displacement
20 mm
Down

Figure S4

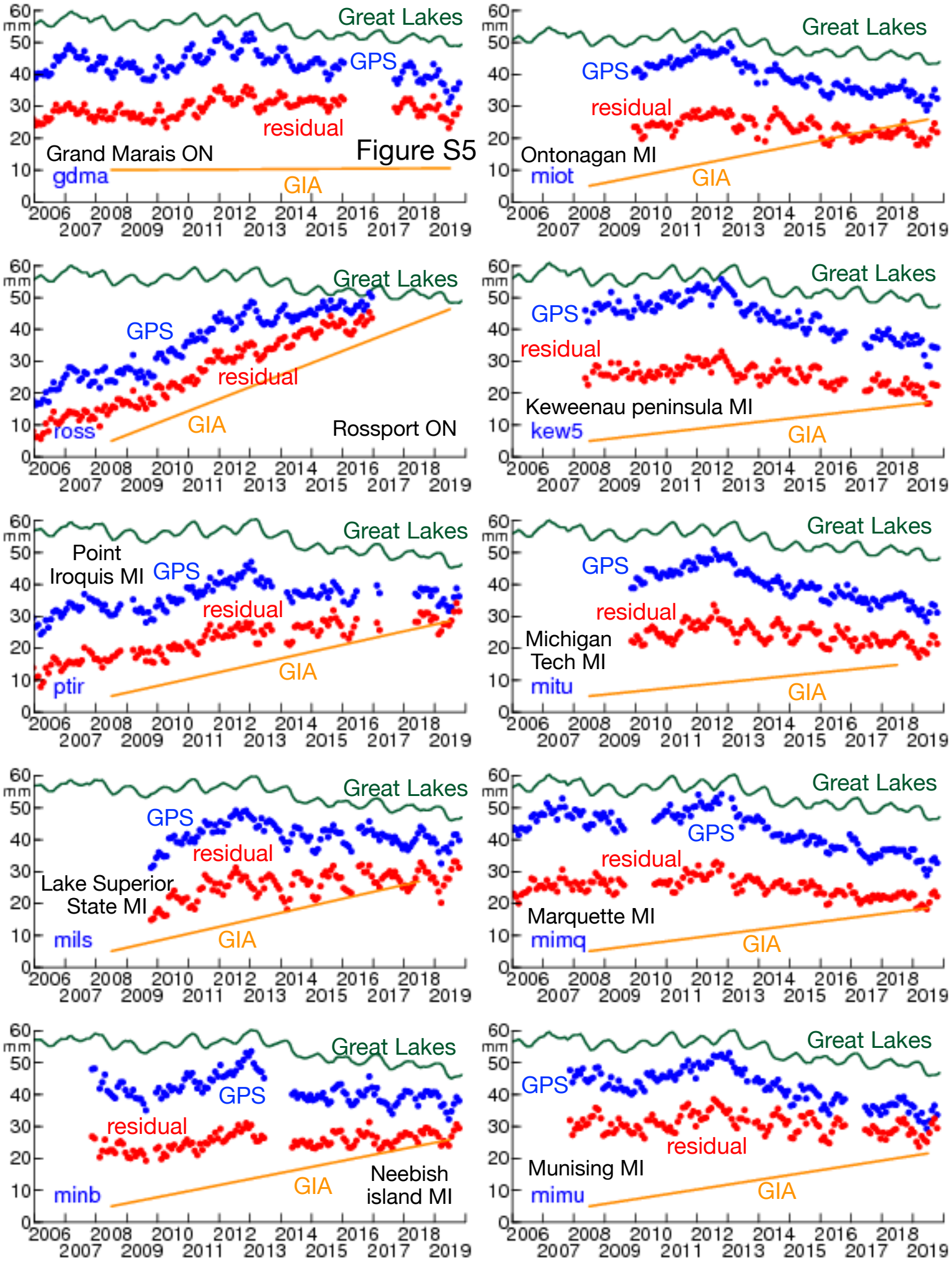
Figure S5
Great Lakes
GPS
residual
GIA
mm
Grand Marais ON
gdma
Ontonagan MI
miot
Rossport ON
ross
Keweenau peninsula MI
kew5
Point
Iroquis MI
ptir
Michigan
Tech MI
mitu
Lake Superior
State MI
mils
Marquette MI
mimq
Neebish
island MI
minb
Munising MI
mimu
2006 2008 2010 2012 2014 2016 2018
2007 2009 2011 2013 2015 2017 2019

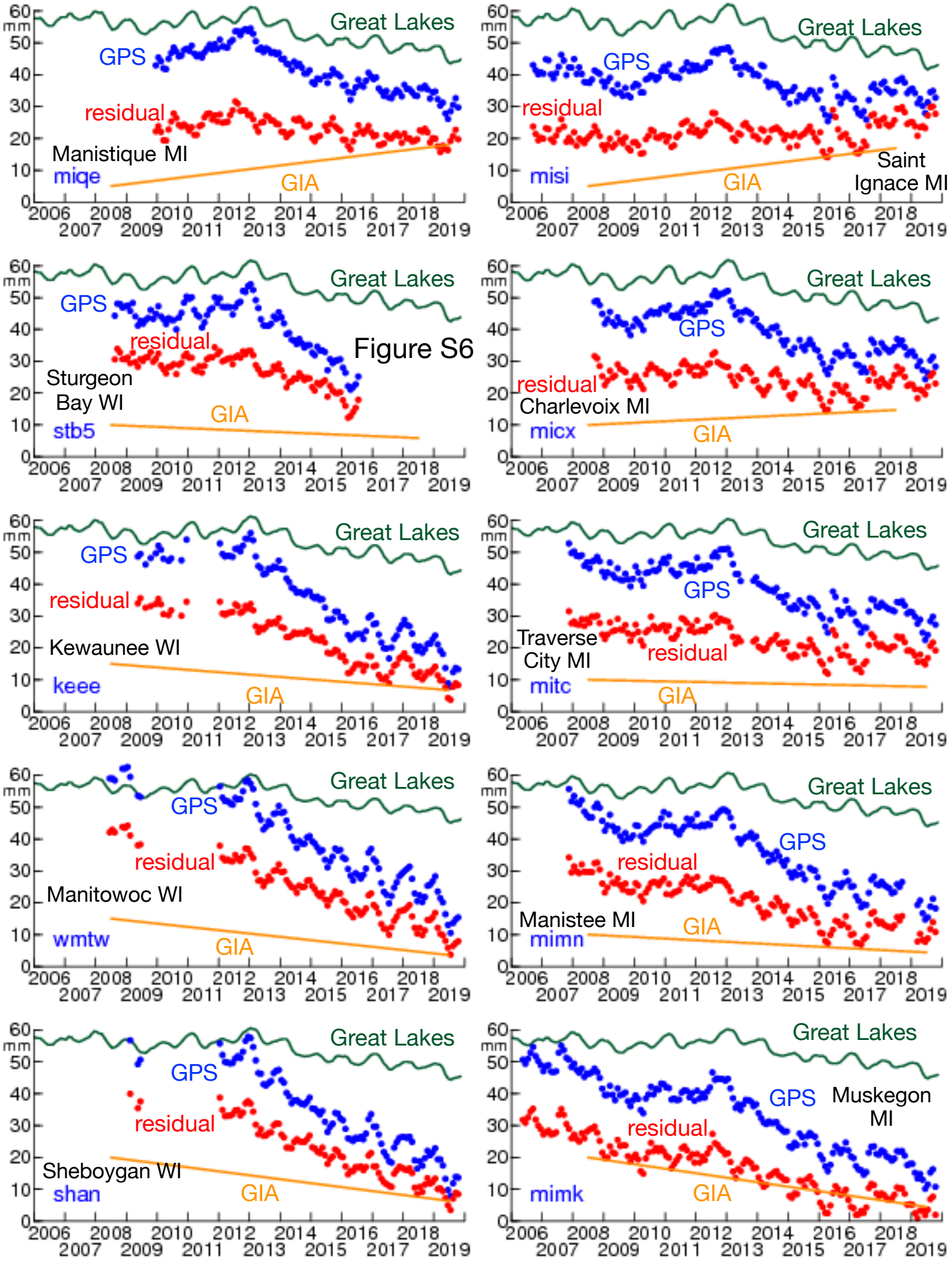
Great Lakes
GPS
residual
GIA
mm
Manistique MI
miqe
Saint Ignace MI
misi
Sturgeon Bay WI
stb5
Figure S6
Charlevoix MI
micx
Kewaunee WI
keee
Traverse City MI
mitc
Manitowoc WI
wmtw
Manistee MI
mimn
Sheboygan WI
shan
Muskegon MI
mimk
2006 2008 2010 2012 2014 2016 2018
2007 2009 2011 2013 2015 2017 2019

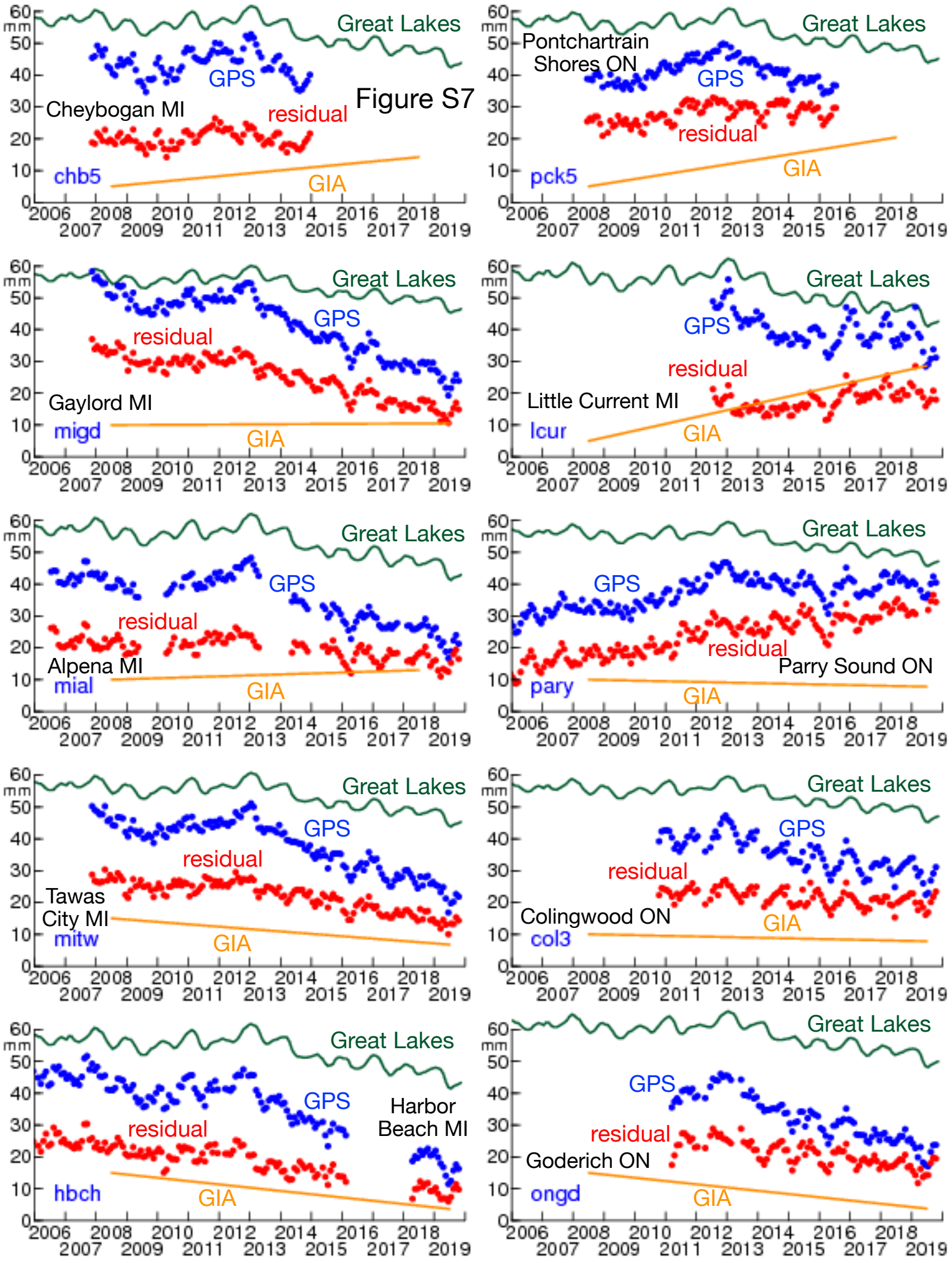
Figure S7
Great Lakes
GPS
residual
GIA
Cheybogan MI
chb5
Pontchartrain Shores ON
pck5
Gaylord MI
migd
Little Current MI
lcur
Alpena MI
mial
Parry Sound ON
pary
Tawas City MI
mitw
Colingwood ON
col3
Harbor Beach MI
hbch
Goderich ON
ongd
mm
2006 2008 2010 2012 2014 2016 2018
2007 2009 2011 2013 2015 2017 2019

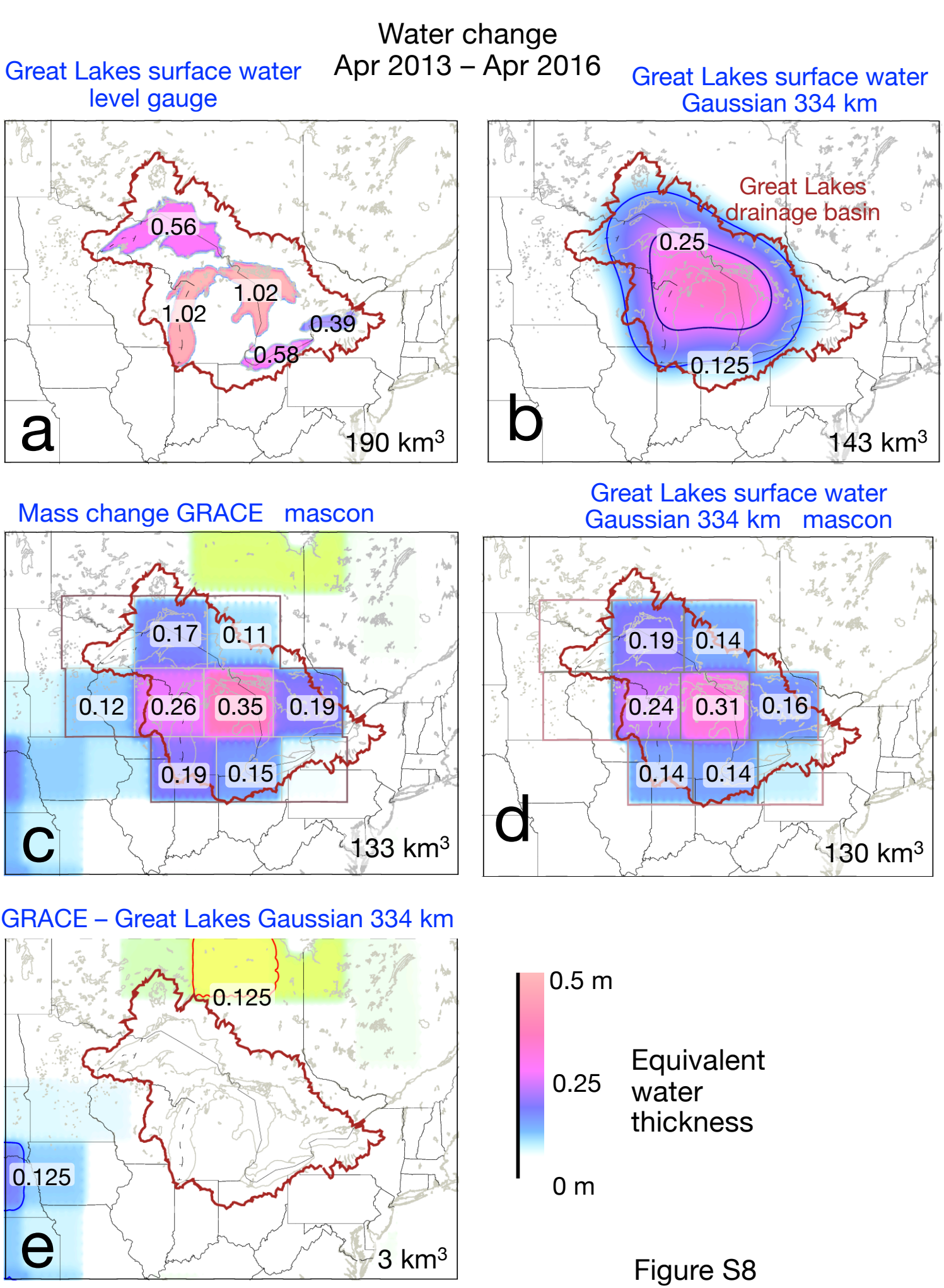
Water change
Apr 2013 – Apr 2016
Great Lakes surface water level gauge
Great Lakes surface water Gaussian 334 km
Great Lakes drainage basin
0.56
1.02
1.02
0.39
0.58
0.25
0.125
a
190 km3
b
143 km3
Mass change GRACE mascon
Great Lakes surface water Gaussian 334 km mascon
0.17
0.11
0.12
0.26
0.35
0.19
0.19
0.15
0.19
0.14
0.24
0.31
0.16
0.14
0.14
c
133 km3
d
130 km3
GRACE – Great Lakes Gaussian 334 km
0.125
0.125
e
3 km3
0.5 m
0.25
0 m
Equivalent water thickness

Figure S8

Figure S9a

Water change
Apr 2013 – Apr 2016

Great Lakes Gaussian

GRACE – Great Lakes Gaussian

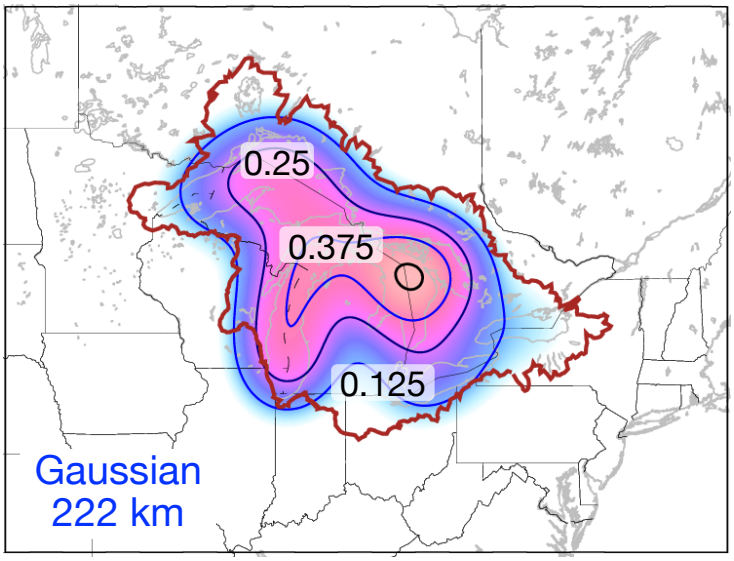

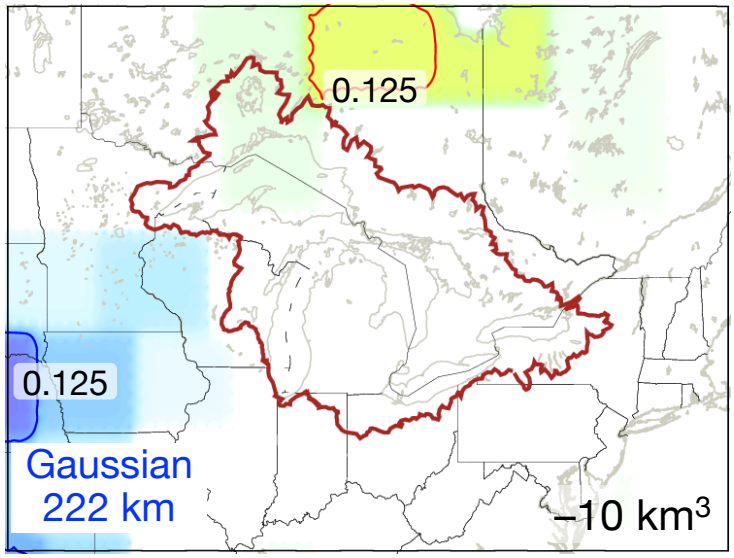

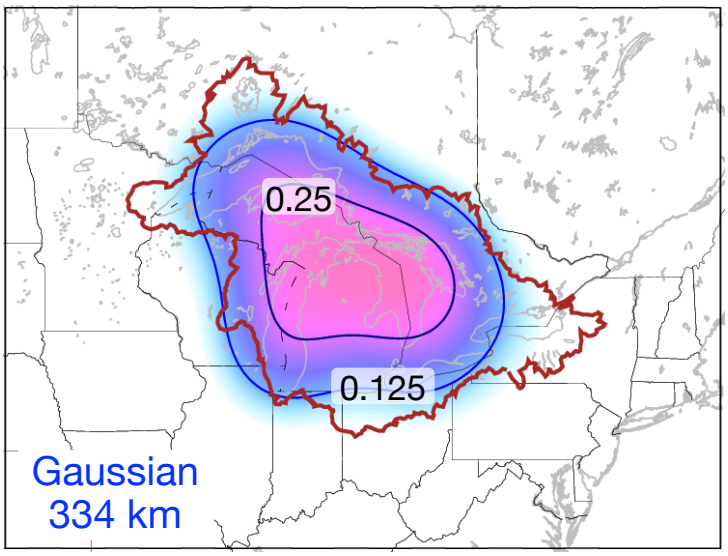

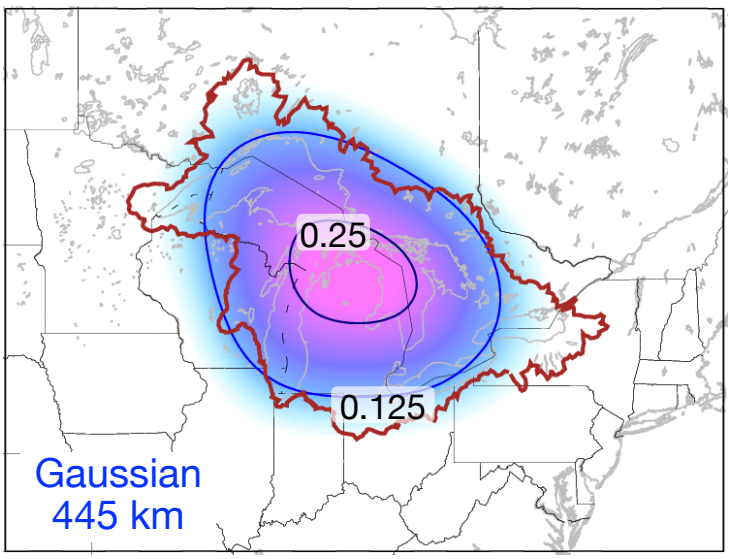

Figure S9b

Water change
Apr 2013 – Apr 2016

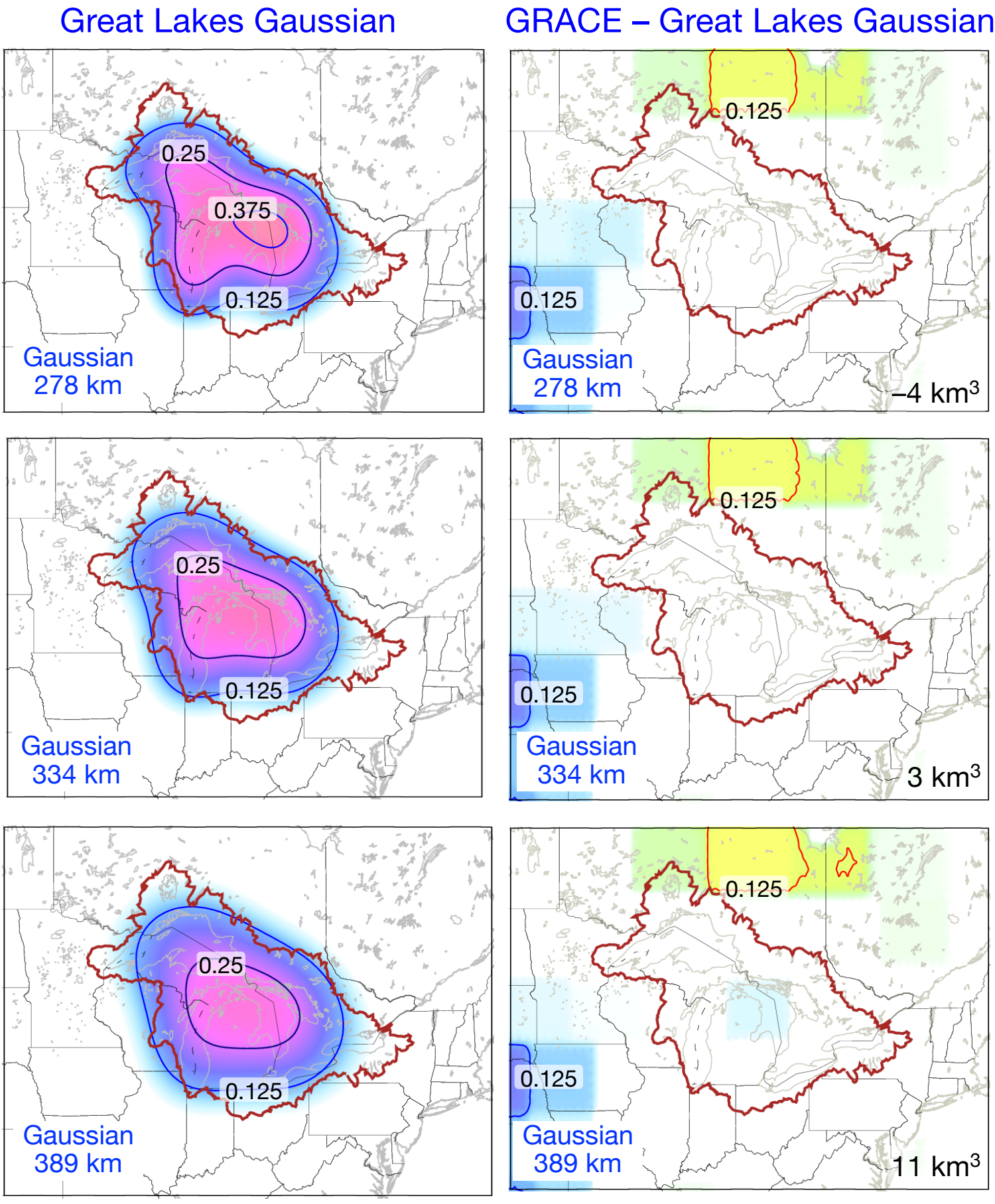

Different areas
to integrate GRACE over

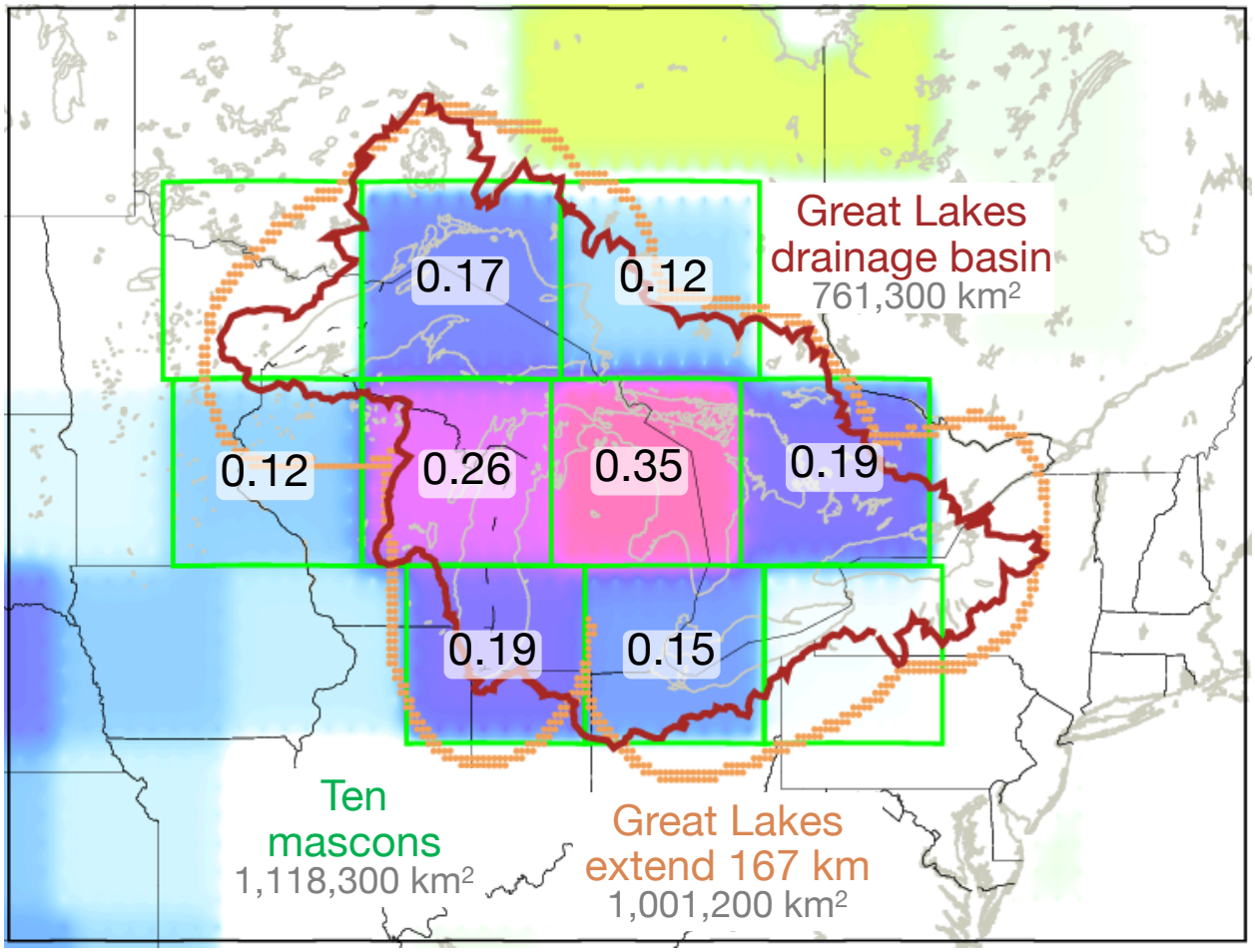

GRACE
Apr 2013 – Apr 2016

Equivalent
water
thickness

Figure S10

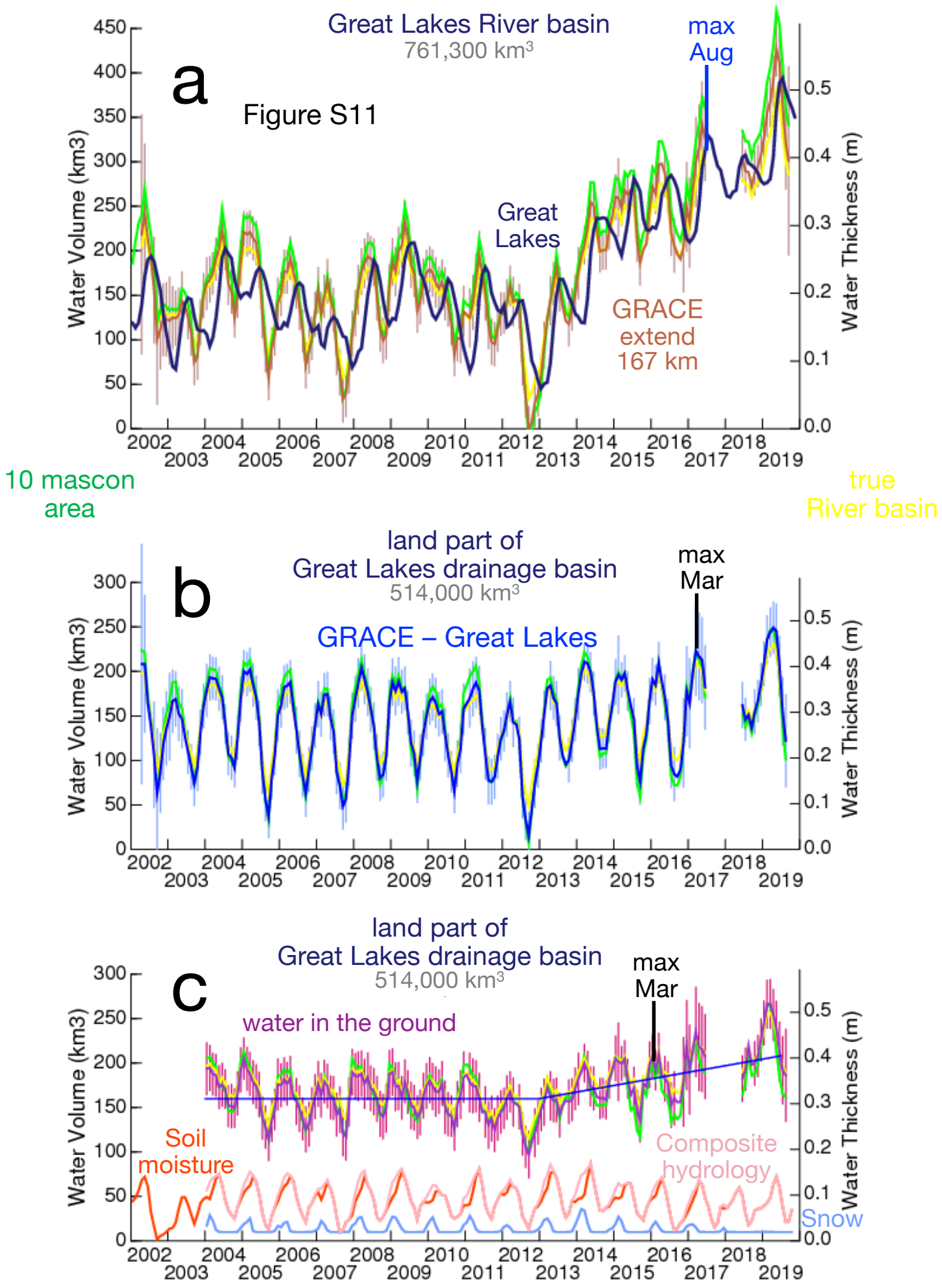
a
Figure S11
Great Lakes River basin
761,300 km3
max
Aug
Great
Lakes
GRACE
extend
167 km
Water Volume (km3)
Water Thickness (m)
10 mascon
area
true
River basin
b
land part of
Great Lakes drainage basin
514,000 km3
GRACE – Great Lakes
max
Mar
c
land part of
Great Lakes drainage basin
514,000 km3
max
Mar
water in the ground
Soil
moisture
Composite
hydrology
Snow

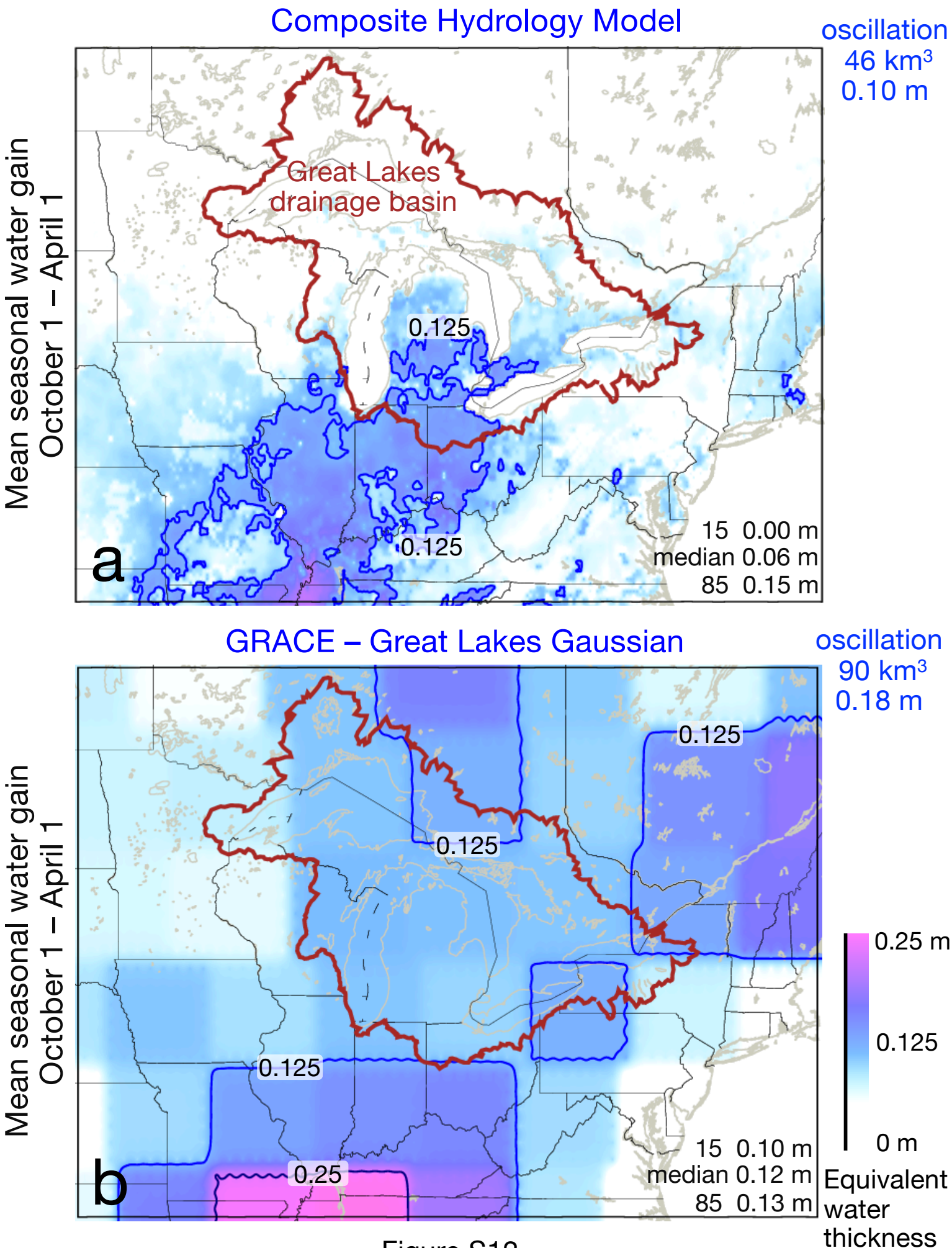
Composite Hydrology Model
oscillation
46 km³
0.10 m
Mean seasonal water gain
October 1 – April 1
Great Lakes
drainage basin
0.125
0.125
a
15 0.00 m
median 0.06 m
85 0.15 m
GRACE – Great Lakes Gaussian
oscillation
90 km³
0.18 m
Mean seasonal water gain
October 1 – April 1
0.125
0.125
0.125
0.25
b
15 0.10 m
median 0.12 m
85 0.13 m
0.25 m
0.125
0 m
Equivalent
water
thickness

Figure S12

GRACE – Great Lakes Gaussian 334 km
Apr 2013 – Apr 2016

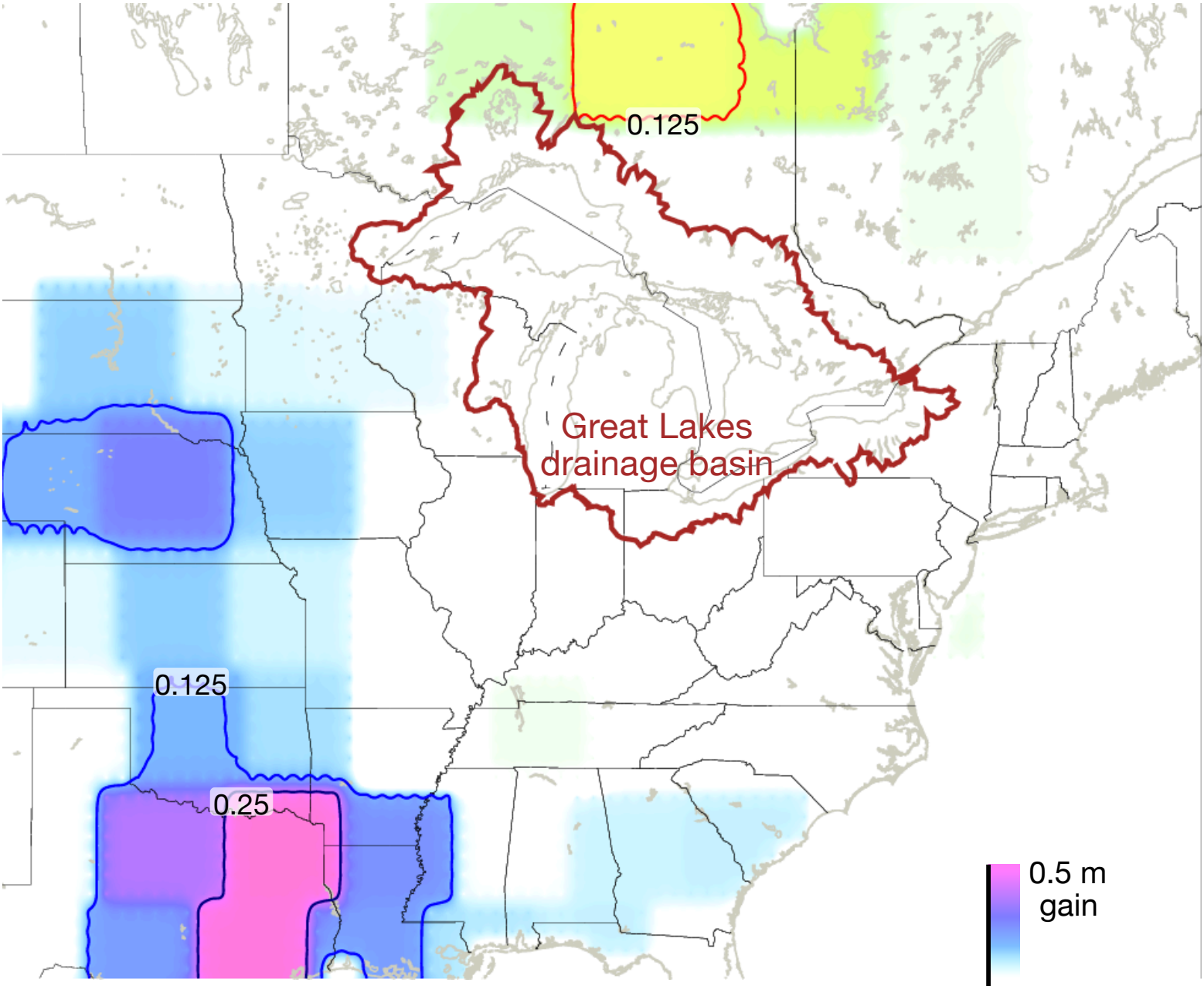

Figure S13

GRACE – Great Lakes Gaussian 334 km
Oct 2012 – Oct 2019

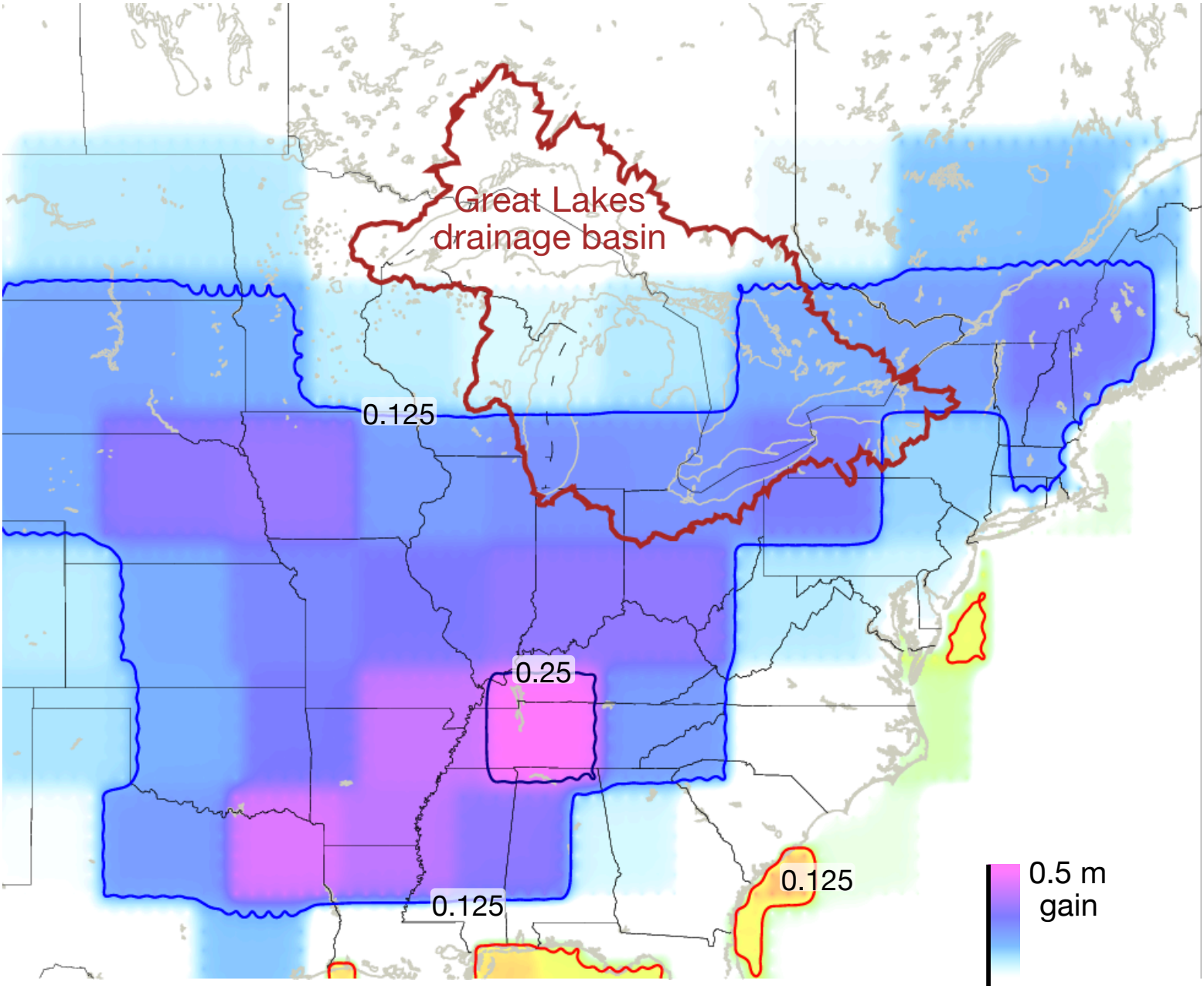

Figure S14

Michigan
seasonal oscillation in
vertical displacement

GPS
elastic
porous
Great Lakes
GRACE

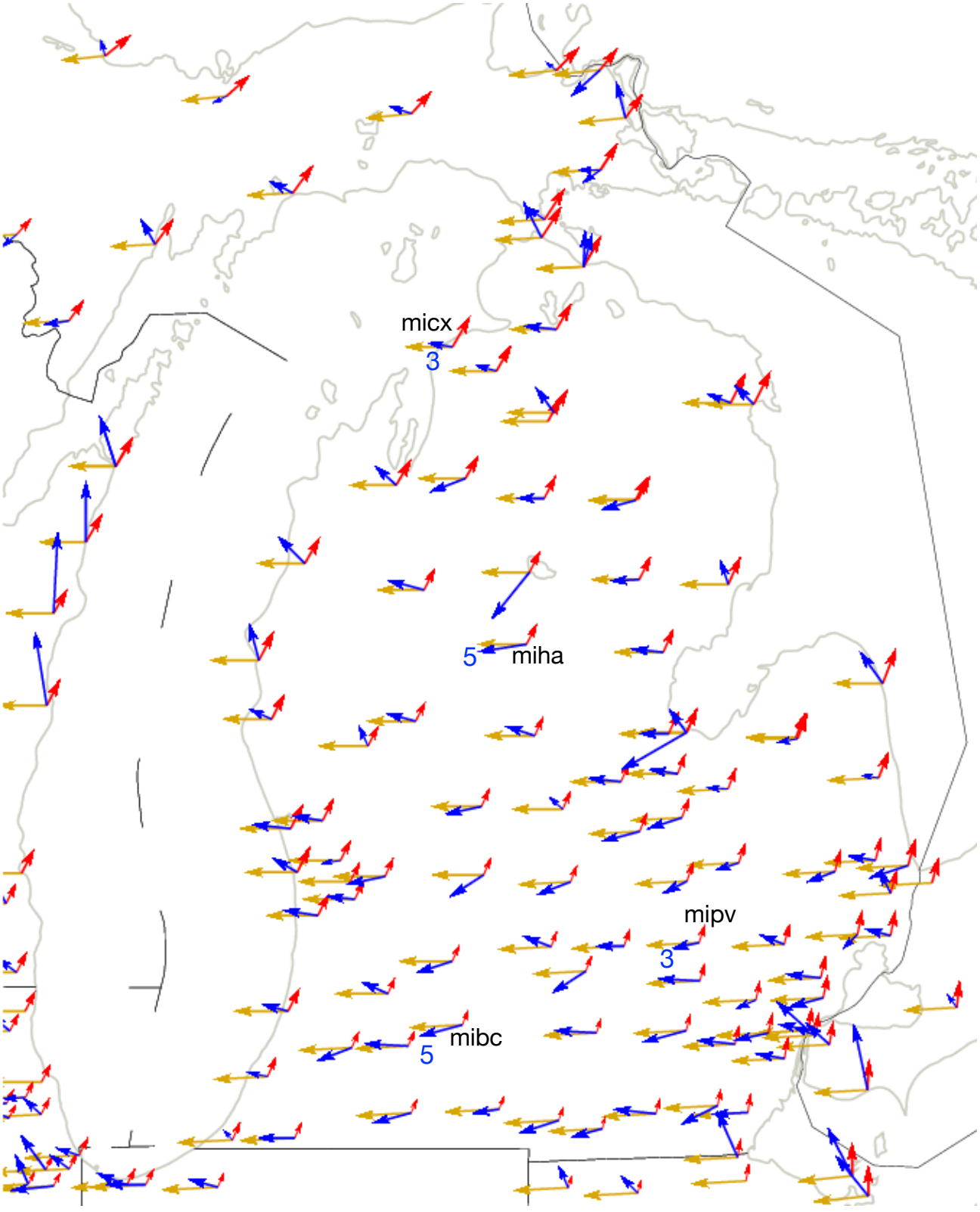

Figure S15a

Wisconsin
seasonal oscillation in
vertical displacement

GPS
elastic
porous
Great Lakes
GRACE

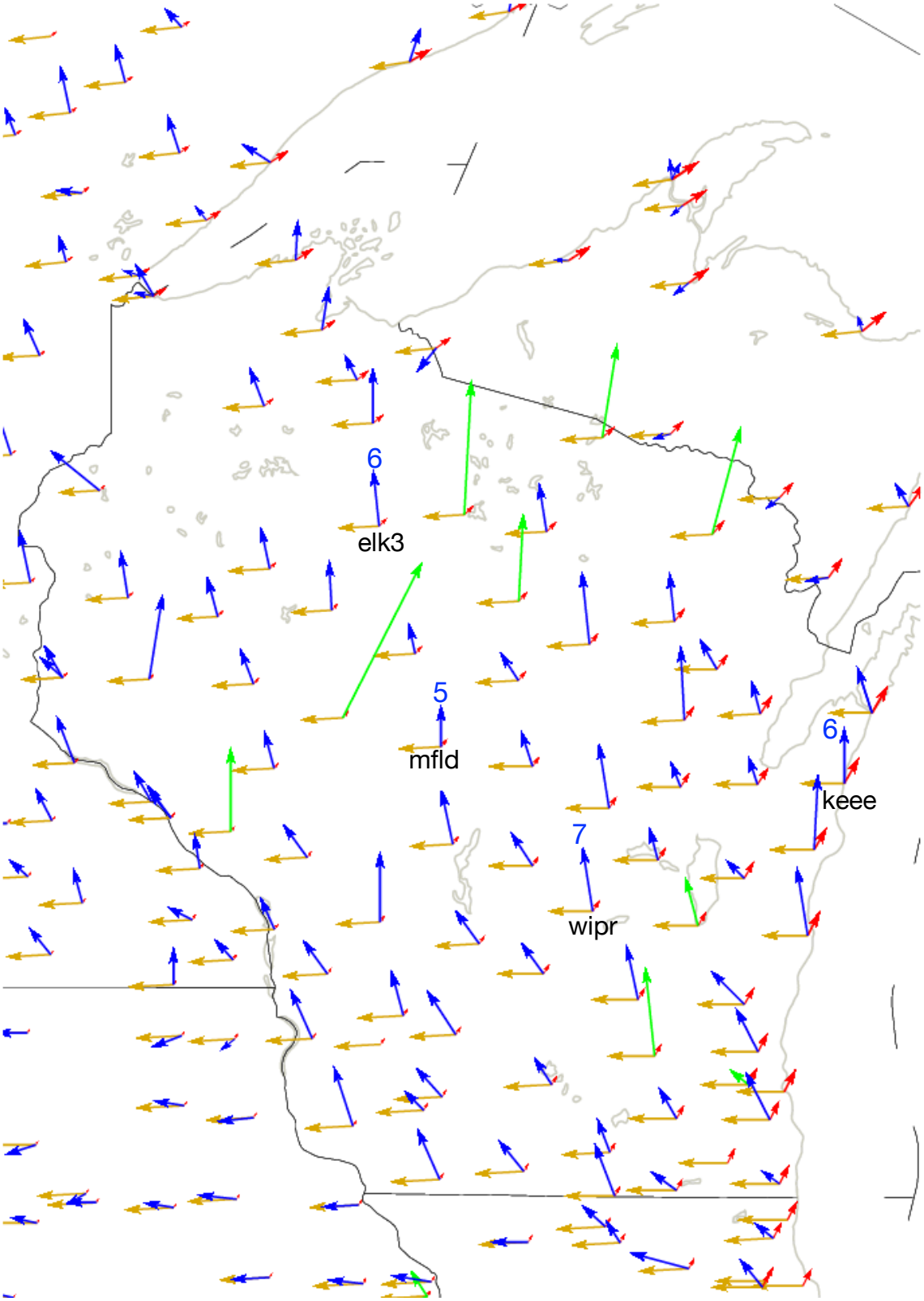

Figure S15b

Michigan
seasonal oscillation in
vertical displacement

Great Lakes
removed
GPS
GRACE
Composite
hydrology

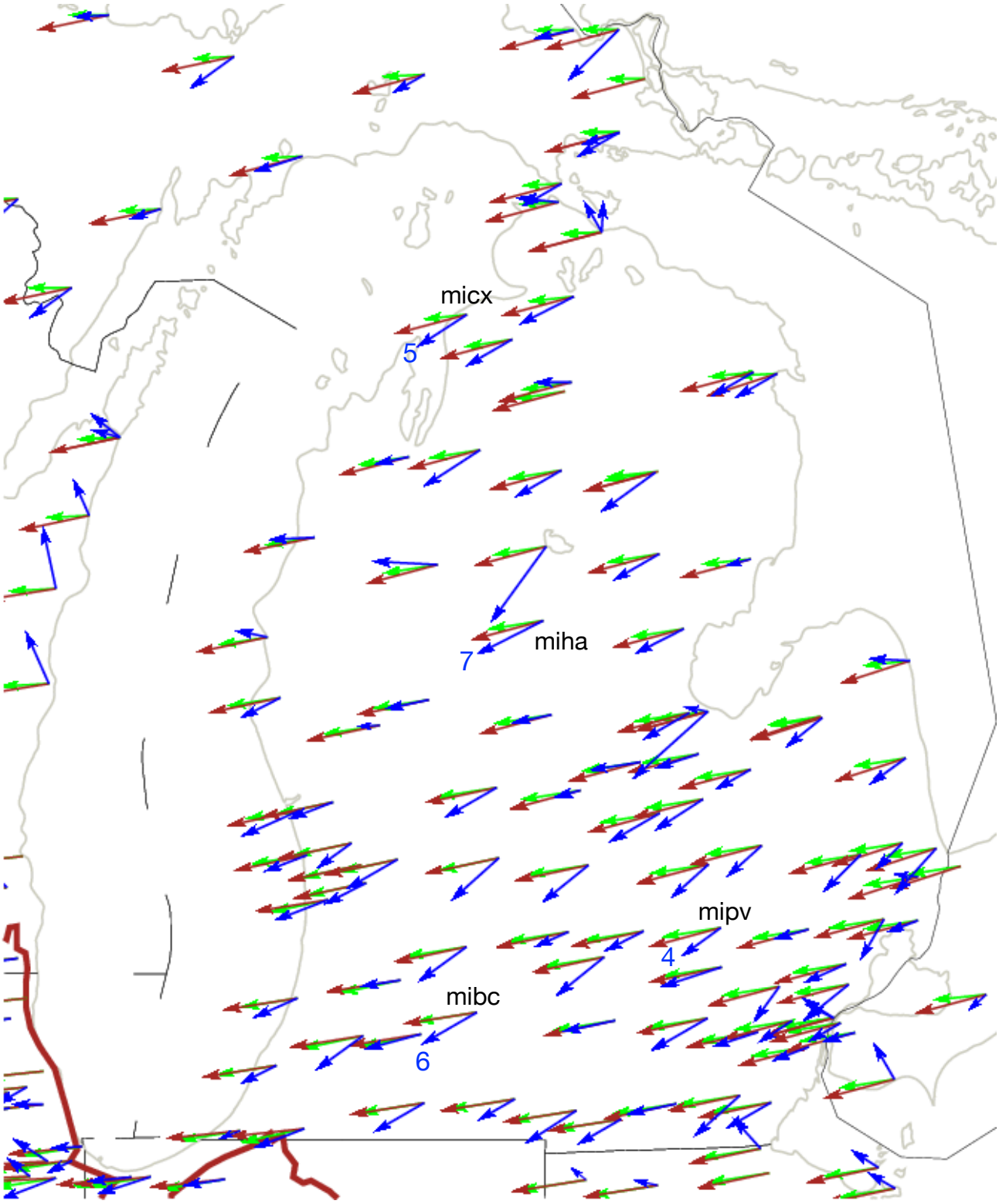

Figure S16a

Wisconsin
seasonal oscillation in
vertical displacement

Great Lakes
removed
GPS
GRACE
Composite
hydrology

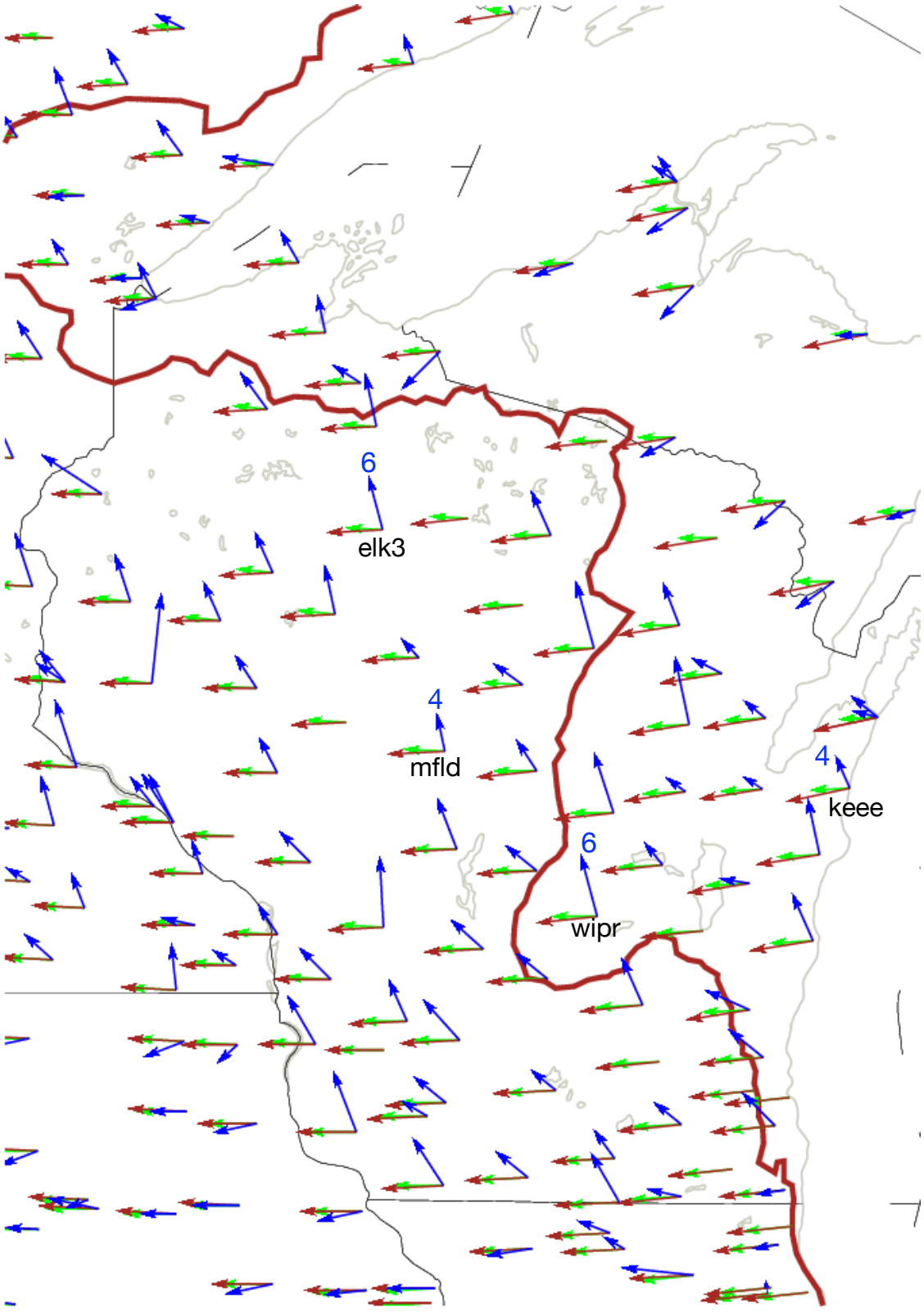

Figure S16b

Mean seasonal water gain
October 1 – April 1
Vs.
Seasonal oscilation in
vertical displacement

Great Lakes removed
GPS
GRACE
Composite hydrology

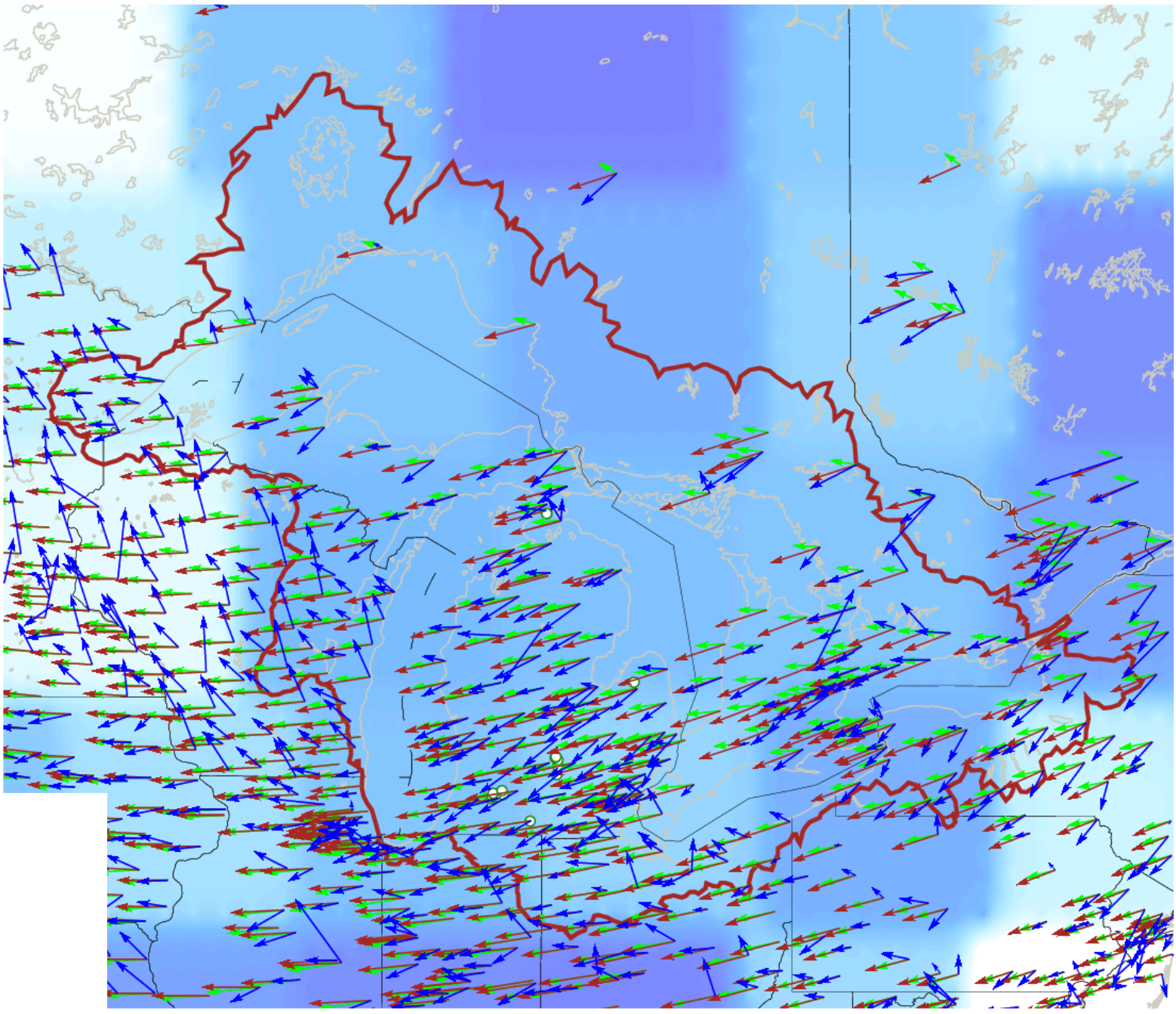

Equivalent water thickness

oscillation 89 km^3 0.20 m

Figure S17